REPORT DOCUMENTATION PAGE

Form Approved
OMB No. 0704-0188

1. AGENCY USE ONLY (Leave blank)

2. REPORT DATE

3. REPORT TYPE AND DATES COVERED

4. TITLE AND SUBTITLE
Lattice and Defect Structures of Polymerizable Diacetylene Langmuir-Blodgett Films Studied by Scanning Force Microscopy

5. FUNDING NUMBERS
Grant N00014-94-1-0270
R & T Code 31321 01
Kenneth Wynne

6. AUTHOR(S)
H. Vithana, d. Johnson, R. Shih, J. Mann, and J. Lando

7. PERFORMING ORGANIZATION NAME(S) AND ADDRESS(ES)
Kent State University, Liquid Crystal Institute & Physics Department, Kent, OH 44242, and Case Western Reserve University, Department of Chemical Engineering and Department of Macromolecular Science, Cleveland, OH 44106

8. PERFORMING ORGANIZATION REPORT NUMBER
8

9. SPONSORING/MONITORING AGENCY NAME(S) AND ADDRESS(ES)
Department of Nayy
Office of Naval Research, 800 North Quincy Street
Arlington, VA 22217-5000

10. SPONSORING/MONITORING AGENCY REPORT NUMBER

11. SUPPLEMENTARY NOTES

12a. DISTRIBUTION/AVAILABILITY STATEMENT
Reproduction in whole or part is permitted for any purpose of the United States Government. This document has been approved for public release and sale; its distribution is unlimited.

12b. DISTRIBUTION CODE

13. ABSTRACT (Maximum 200 words)
The Scanning Force Microscope has been used to study the lattice and defect structures of multilayers of the unsaturated fatty acid, 12-8 diacetylene (10,12-Pentacosadiynoic Acid) in ambient conditions. Films were prepared by the Langmuir-Blodgett technique on ordinary microscope glass and Indium Tin Oxide coated glass. Lattice structures were deduced from the well resolved molecular images and before polymerization found to be nearly centered rectangular with lattice parameters (0.88 ± 0.06)nm and (0.51 ± 0.04)nm. After exposing to UV radiation for polymerization the lattice structure changed to an oblique lattice with lattice parameters (0.466 ± 0.008)nm and (0.55 ± 0.01)nm. Molecular level defects such as dislocations and grain boundaries were resolved in these films very clearly. Observation of these kind of defects implies that it is possible to reliably image the real surface molecules under ambient conditions. Polymerization was found to take place in one of the lattice directions and the modulation perpendicular to that direction was more pronounced than along the polymer backbone.

14. SUBJECT TERMS

15. NUMBER OF PAGES

16. PRICE CODE

17. SECURITY CLASSIFICATION OF REPORT	18. SECURITY CLASSIFICATION OF THIS PAGE	19. SECURITY CLASSIFICATION OF ABSTRACT	20. LIMITATION OF ABSTRACT
unclassified	unclassified	unclassified	

. . To appear in 6/75 issue of JVST-B

LATTICE AND DEFECT STRUCTURES OF POLYMERIZABLE DIACETYLENE LANGMUIR-BLODGETT FILMS STUDIED BY SCANNING FORCE MICROSCOPY

Hemasiri Vithana[a], David Johnson[a], Raymond Shih[b], J. Adin Mann, Jr[b] and Jerome Lando[c]

Liquid Crystal Institute and Department of Physics[a]
Kent State University
Kent, Ohio 44242

Department of Chemical Engineering[b]
Case Western Reserve University
Cleveland, Ohio 44106.

Department of Macro Molecular Science[C]
Case Western reserve University,
Cleveland, Ohio 44106.

ABSTRACT

The Scanning Force Microscope has been used to study the lattice and defect structures of multilayers of the unsaturated fatty acid, 12-8 diacetylene (10,12-Pentacosadiynoic Acid) in ambient conditions. Films were prepared by the Langmuir-Blodgett technique on ordinary microscope glass and Indium Tin Oxide coated glass. Lattice structures were deduced from the well resolved molecular images and before polymerization found to be nearly centered rectangular with lattice parameters (0.88 ± 0.06)nm and (0.51 ± 0.04)nm. After exposing to UV radiation for polymerization the lattice structure changed to an oblique lattice with lattice parameters (0.466 ± 0.008)nm and (0.55 ± 0.01)nm. Molecular level defects such as dislocations and grain boundaries were resolved in these films very clearly. Observation of these kind of defects implies that it is possible to reliably image the real surface molecules under ambient conditions. Polymerization was found to take place in one of the lattice directions and the modulation perpendicular to that direction was more pronounced than along the polymer backbone.

INTRODUCTION

Ultra-thin two dimensionally ordered organic molecular films can be prepared using the Langmuir-Blodgett (LB) technique[1]. A major drawback of LB films in any application is their lack of mechanical stability. To overcome this problem utilization of polymerizable materials in LB film preparation has gained wide acceptance. Two basic methods used are[1]: (1) a polymerizable monomer is spread onto the water-air interface and polymerization is induced before or after transferring the film to the substrate or (2) a preformed polymer is spread onto the water-air interface and transferred to the substrate. In the latter method difficulties can arise in transferring the film to the substrate due to film rigidity. Polymerizable LB films which are commonly used are those with one or more double bonds, with diacetylene groups and with oxirane groups. A detailed description of these families is given in reference (1) and (2). Polymerization of LB films made from unsaturated fatty acids can be initiated by UV or γ radiation or by heat treatment. Among the unsaturated fatty acids studied as LB films, diacetylene derivatives have gained the most attention due to their mechanical rigidity upon polymerization. They have two conjugated triple bonds and can be readily polymerized by UV radiation, giving rigidity to the film; which, however , may develop defects, cracks and grain boundaries[3].

The availability of a variety of organic molecular materials which can form LB films and the fact that the molecular structure

of these materials can be readily modified have led to many applications and the number is growing rapidly. Molecular electronics, optoelectronics, non-linear optics, semiconductors and chemical/biological sensors are some of the major areas of applications. For all these it is important to have defect free homogeneous LB films; therefore it is necessary to characterize these films experimentally. Molecular ordering of LB films and their properties have been studied by many experimental techniques[1], such as X-ray diffraction, electron diffraction, ellipsometry, electron and optical microscopy, various spectroscopies and more recently by (SPM) Scanning Probe Microscopy [4-9]. Compared to other techniques, SPM has the ability to visualize the lattice structure in real space and identify defects on the scale of a molecular length. Characterization of diacetylene LB films has been studied by x-ray and electron diffraction[10], fluorescence microscopy[4] and (SFM) Scanning Force Microscopy[11,12]. In this article we report the results of detailed SFM observations of lattice structures of 12-8-diacetylene acid LB films in monomeric and and polymeric forms and of different types of defects present in the films.

To scan the soft surfaces of LB films non-destructively by SFM it is necessary to keep the operating force at a minimum. The theoretical predictions are lower than the actual forces acting between the tip and the sample when scanning in air[13,14]. Experimentally, in air, it is not possible to obtain operating forces close to theoretical values even with the sharpest tips commercially available. Thus the question of whether we are

imaging real molecules or artifacts remains unanswered. This problem is addressed by considering the defect structures observed in these films.

EXPERIMENT

Substrates used in this study were ordinary microscope glass and Indium Tin Oxide (ITO) coated glass. Over an area of $(500x500)nm^2$ the RMS roughness of the substrates are 6.5 ^0A and 4.2 ^0A, respectively as measured by SFM. There was no particular reason for using ITO coated glass in this study other than its different RMS roughness and surface material compared with that of ordinary microscope glass.

The maximum length of the 12-8-diacetylene molecule is 2.96 nm[15]. The diacetylene monomer was spread onto the subphase, an aqueous solution of 10^{-3} $CdCl_2$ in pure water with pH adjusted to 7 by adding NaOH. LB films were transferred to substrates at a temperature of 20 ± 1 ^0C at a surface pressure of 30 mN/m and 0.2 nm^2/molecule by vertical dipping. The dipping speed was 2 mm/min and the transfer ratio was close to unity for both up and down depositions. Samples used in this study were Y-type, where packing order is head-to-head and tail-to-tail, with an odd number of layers on the hydrophobic substrates. Hence, end methyl groups of the top most layer are exposed to the air.

A Digital Instruments Nanoscope III SFM was used to image the samples under ambient conditions on a vibration isolation system. Scan Head A (maximum scan size 0.7x0.7 μm^2) and pyramidal silicon nitride tips (force constant ~ 0.06 N/m) were used for all the scans, and the forces between the tip and the sample were approximately

5 nN or less. The SFM was used in the deflection mode where the sample is held at constant height, z, and the cantilever deflection is monitored during x-y scanning. For these images scanning rates of 61 Hz with 512x512 pixels and 122 Hz with 256x256 pixels were used. All the images presented are unprocessed, ie, no filtering was applied, except where indicated. Images were obtained in many locations and scanned in different directions. To obtain reliable lattice parameters, it was necessary to calibrate the SFM head first, allowing sufficient time to eliminate thermal and mechanical drifts before capturing an image. For this we used mica. Eight images from different locations and areas ranging from (50x50) nm^2 to (12x12) nm^2 were captured.

Observation of the positions (distance from the center and angle) of intense spots at the reciprocal lattice sites in the 2D-Fourier spectrum of molecular resolved images of the LB film samples captured from the same location gave the following information. Variation of these parameters between up and down scans revealed any drift during scanning. Variation with scanning force showed whether the lattice structure was sensitive to the measuring force. To check the effect of drift while scanning, 30x30nm^2 images were captured from the same location on a 9 layer diacetylene LB film, for both up and down scanning, every 5 minutes for 35 minutes. To investigate the effect of force on the sample, images from the same location were captured with varying forces. Each image was captured after~20 minutes of scanning at each force. Both up and down scanned images were captured. The force was varied from 2 to 12 nN. However, scanning with a 2 nN force was not stable; the tip jumped away from the sample most of the time. Several tips were used in the experiment.

Three monomer samples, two with 9 layers, one on an ordinary microscope slide and the other on an ITO coated glass substrate, and one with 15 layers on an ITO coated glass substrate were used. After analyzing these monomer samples with the SFM, they were polymerized by exposing to unpolarized UV radiation (λ~254 nm) for further analysis. All the images were captured after 20-25 minutes of scanning at the same location. Because of the difficulty of the tip jumping away from the sample surface with low operating forces (2 nN), we set the force between the tip and the sample at approximately 5 nN. To compute the lattice parameters, the raw image was first Fourier filtered. Keeping only the intense spots in the 2D-Fourier spectrum, the repeat distances were measured in the regenerated real space image at more than one position. This procedure was repeated for many images captured from different locations and averaged to compute the final value and uncertainties of the lattice parameters. Specifically sixteen images captured from seven different locations of the monomer films and eleven images captured from five different locations of the polymerized films were used. The error bars were taken as the standard deviations of the above measurements.

RESULTS

The molecular resolved images of mica captured for the head calibration gave the following results. Average values of the reciprocal lattice vectors (RLVs) and the angles between two adjacent RLVs were obtained from the 2D-Fourier Spectrum; they are 2.235 ± 0.015, 2.244 ± 0.02, and 2.246 ± 0.015 nm^{-1} and 60.2 ± 0.4, 59.08 ± 0.7, and 60.0 ± 0.6 degrees respectively. From the Fourier filtered images the

value obtained for the repeat distance of the hexagonal lattice structure of mica is 0.516 $\pm$ 0.004 nm which agrees very well with values reported previously [16]

While checking the effect of the drift, the force between the sample (polymerized LB film of 9 layers) and the tip was set at ~ 5 nN and the scan rate was set at 61 Hz for 256x256 pixel resolution. At this fast scan rate, the RLVs and the angles of the intense spots in the 2D Fourier spectrum between up and down scans became stable within the limits of measurements after 20-25 minutes of scanning. After 15 minutes of scanning, the maximum observed variations in the RLV and in the angle were $0.043 nm^{-1}$ and 3.4^0, respectively. After 25 minutes of scanning, this dropped down to $0.014 nm^{-1}$ and 0.8^0, and no significant improvements were observed by further increasing the scanning time. Within the range of forces used (2 to 12 nN) for checking the effect of the force, we did not observe any visible damage to the sample. For large scan areas, $30x30 nm^2$, with a scan rate of 61 Hz and 256x256 pixel resolution, the maximum observable variation with force in RLVs was $0.036 nm^{-1}$ and 3.67^0 in angle. For small scan areas, $12x12 nm^2$, with 256x256 pixel resolution and 122 Hz scan rates, the maximum variation with force in RLVs was $0.008 nm^{-1}$ and 1.82^0 in angles. At higher forces we observed 0.5-0.8 nm z-direction corrugations while at lower forces this dropped down to (0.2-0.3) nm. It has been shown that the frictional force between the tip and the sample increases with the operating force, thereby increasing the corrugation height[17]. LB films are soft and the tip is moving on or through the methyl groups of the alkyl chains of the molecules. At large forces it is possible that the tip may penetrate through the chains.

Molecular resolved images were obtained in areas as large as $70x70\ nm^2$. However, even in $30x30\ nm^2$ scans defects were visible through the 2D Fourier spectrum. These defects are mainly domain boundaries. The change in direction of the lattice rows is more pronounced when Fig.1(a) is viewed at a glancing angle and slowly rotated. Therefore, to compute the lattice parameters we chose smaller areas.

Monomer Samples:

Fig.2(a) and (b) show an unprocessed image of a $5x5\ nm^2$ area and its 2D-Fourier spectrum, respectively, and Fig.2(c) shows the 2D-Fourier spectrum of an image of a $16x16\ nm^2$ area obtained from the same 9 layer sample. Fig.2(d) is a schematization of 2(c) with Miller indices (h&k) indicated. The 2D-Fourier spectrum implies that the real space lattice is centered rectangular with 2 molecules per unit cell. The six strong spots (large filled circles) correspond to even values of (h+k). The origin of the less intense spots (open circles) could be due to a buckling super-structure in the film similar to observations by Garnaes et al[4] in their Cadmium Aracidate LB films, or could correspond to the odd values of (h+k) which would indicate that the lattice is not a perfectly centered rectangular. Since we do not see any buckling structure in the real images and no satellite spots corresponding to sum and difference of the wave vectors for the buckling and the molecular lattice, we conclude that these corresponds to odd values of (h+k); however, they are not very strong.

The RLVs corresponding to the intense spots and the angle between adjacent RLVs are 2.38 ± 0.05, 2.29 ± 0.63, and $2.13 \pm 0.7\ nm^{-1}$ and 61 ± 1, 65 ± 1, and 54 ± 1^0 respectively. Here two of the RLVs and the angles are nearly equal indicating that this

is a nearly centered rectangular lattice. From these measurements we deduced the unit cell shown in Fig.3. Electron diffraction patterns obtained from 12-8 diacetylene[10] were very similar to those from polyethylene single crystals and indicate that the zig-zag planes of the alkyl chains of the neighboring diacetylene molecules are oblique with respect to each other. Because of this the methyl end groups of the diacetylene molecules, which the SFM tip probes, are not in an exact centered rectangular unit cell. This is the same as the unit cell observed in Cadmium Aracidate LB films by SFM[4,5]. Lattice parameters obtained for the unit cell are $a = 0.51 \pm 0.04$ nm and $b = 0.88 \pm 0.06$ nm, higher than obtained previously by electron diffraction on 20 layer LB films deposited at a pressure of 20 mN/m[10], namely a= 0.486 nm and b = 0.740 nm (error bars are not given). Positional correlation of the molecules in these images extended well over 10 nm in all lattice directions as shown in Fig.4.

Polymerized Samples:

After UV exposure the samples became pink which is a signature of polymerization[15]. For polymerization to occur, diacetylene molecules have to be arranged with proper distances from one another. Evidently this arrangement is present in our LB films. Previous studies have shown that the quality of the polymer films depend on the molecular structure of the diacetylene acids[18,19].

Earlier we showed that the layer thickness decreased by~10% and the topography and the roughness changed upon

polymerization[15]. Fig. 5 shows a molecular resolved image and 2D-Fourier spectrum of a polymerized 9 layer film. From this image it is clear that the lattice structure changed upon polymerization. In the Fourier spectrum, spots due to the odd values of (h+k) are not present and the spots due to (1,1) and $(\bar{1}, \bar{1})$ are very weak compared with monomer films. Thus a nearly rectangular lattice changed into an oblique lattice. After averaging over all the images we obtained the following lattice parameters: $a = 0.466 \pm 0.008$ nm , $b = 0.55 \pm 0.01$ nm and $\theta = 100 \pm 2^0$. These values again are a little higher than the previously reported values[10], $a = 0.43 \pm 0.01$ nm and $b = 0.49$ nm, where the LB films were deposited at pressure of 20mN/m. As can be seen, the Z-direction amplitude is more pronounced in one lattice direction than in the other. The distance between the more pronounced rows is 0.54 ± 0.01 nm and, as we explained in our previous paper[15], we interpret this as the distance between the polymer backbones. Consistent with earlier studies[10,20], after polymerization the polymer backbone should be along the (0,1) direction with respect to the monomer lattice. The inplane packing changes from herringbone (Fig.3) to uniaxial oblique. Fluorescent microscopy and SFM studies[11,20] have also shown that the 12-8-(poly)diacetylene polymer backbone is along a monomer lattice direction. Furthermore, a change in lattice structure upon polymerization has been observed in LB films prepared with other kinds of unsaturated fatty acids[6], and suggests that the position of the reactive bonds in the hydrocarbon chains could be partly responsible for causing a change in molecular tilt upon polymerization which in turn may cause the change in molecular ordering. Unlike those studies we did not see any decrease in the molecular ordering only that it is different from that of monomer films. The 2D autocorrelation image

of a polymerized sample presented in Fig. 6 shows that molecular order in both lattice directions is present for well over 15 nm. By looking at a glancing angle this is clearly visible in the direction nearly perpendicular ($\theta=100^0$) to the polymer backbone direction.

Defect Structures:

The ability to observe molecular scale defects is one of the main advantages of SFM. We observed both large and molecular scale defects in all the LB film samples studied. Same kind of defects are present before and after polymerization. Pin hole type defects varying in diameter from a few nanometers to a few micrometers have been observed in many LB films[7]. Also it is possible to create pin hole type defects by scanning with a high operating force between the tip and the sample[8]. These defects are a function of the type of substrate used, roughness of the substrate, film aging, subphase conditions, transfer process and the scanning process itself.

In this article we report on the three types of defects observed in our samples: grain boundaries, edge and screw dislocations. Grain boundaries can be easily detected by analyzing the 2D-Fourier spectrum. As Shown in Fig.1(b), there exists more than 1 set of spots on one side of the image indicating more than one distinct lattice direction. By decreasing the scan area we get a better visual picture of the grain boundaries. Fig. 7 shows such an image and its 2D-Fourier spectrum obtained from a 9 layer monomer sample. It is clear in this image that the (0,1) lattice direction has a kink. The Fourier spectrum shows two spots corresponding to the two lattice directions, while the (1,0) lattice direction is uniform. The row of molecules at the grain boundary

is less well resolved compared to the other rows of molecules. The domains are misoriented by an angle of~9^0.

Fig. 8 shows the presence of edge dislocations obtained from a 9 layer monomer sample. To enhance these features, the image was Fourier filtered keeping only the intense spots in the 2D-Fourier spectrum. Because of the two dislocations present here a feature similar to a low angle grain boundary has formed at the middle of the image. The presence of pairs of dislocations with opposite Burgers vectors have been reported earlier and the suggestion was made that this requires a finite energy; whereas isolated dislocations are rare due to the macroscopic elastic energy required[5,9].

The other class of defects we observed were screw dislocations in polymerized samples as shown in Fig.9(a). The terminus of the boundary between the slipped and unslipped part of the film marks the screw dislocation. Fig.9(b) shows the cross-sectional profile across a screw dislocation and the height of the slipped film is 5.613 nm which is very close to the bilayer height. The origin of these dislocations could be related to the mismatch of lattice spacings at grain boundaries of molecules or to the change in lattice parameters during polymerization.

DISCUSSION

Interpretation of images of soft surfaces by SFM has been difficult due to the relatively high force between the tip and the sample. This has been discussed by many researchers. Ohnesorge et, al,[21] have suggested

that high operating forces could be the reason for the lack of laterally well defined atomic scale defects observed in SFM images compared with Scanning Tunneling Microscope (STM) images. They suggested that to obtain true atomic resolution the loading force exerted on the sample by the tip should be around 0.1 nN or lower. It is possible that scanning with a high force may remove the defects from the surface and make it well ordered or that the SFM will image artifacts as a result of piercing through the soft surface. Earlier studies predicted that the resolution obtainable by SFM on soft surfaces is several nanometers[22,23] and that to scan soft surfaces in a non-destructive manner the force should be in the range of 0.01 nN[13] compared with 1-10 nN for hard surfaces[24]. Forces in the 0.01 nN range are not possible operating in air. Also it was suggested that to obtain molecular resolution by SFM, a non-negligible repulsive force is necessary, because molecular distances can be resolved only by repulsive forces[23]. It is possible to decrease the operating force by using very sharp tips with radii of curvature around ~ 10 nm at the apex; which are now commercially available. The manufacturers claim that it is more probable that these tips contain a single atom at the apex than conventional pyramidal tips. By operating the SFM under liquid with these ultra-sharp tips, forces of 0.01 nN have been obtained[21]. However, molecular dynamics calculations show that a single-atom tip can be permanently damaged with a much lower operating force than used in actual experiments performed under liquid[14]. Therefore, experimental results obtained so far were most likely imaged by polyatomic tips. In fact, we tried these ultra-levers in our experiment, but good quality molecular resolved images were

obtained only with the pyramidal tips. When the SFM is operating in contact mode the inelastic deformation limit decreases as the tip gets sharper[22]. Hence damage to the sample could be quite possible even with a very low force, thereby losing the resolution. Therefore, tip shape and the material may also play an important role in obtaining molecular resolved images, and depending on the surface some tips may work better than others.

Previously reported results on soft surfaces, especially on LB films, showed that with operating forces of a few nN it is possible to scan non-destructively at molecular resolution[4,15]. Also from molecular resolved images of Cadmium Aracidate LB films recorded on up and down and back and forth scans, it is clear that SFM is actually imaging the surface molecules[25]. The authors explained this observed molecular resolution by assuming that the tip has a roughness of molecular scale which will give single atomic mini tips with the operating repulsive force distributed non-uniformly over a large area of the sample. Another reason could be that when the number of deposited LB layers increases the surface becomes crystalline and locally atomically smooth. The underlying head-group head-group interaction of the fatty acid molecules is the driving force for this molecular ordering of the surface[26]. Molecular resolved images by SFM are then quite possible on such surfaces, most probably because such surfaces are not very soft. Also it is possible that a tip may not be exactly spherical at the apex, hence it is difficult to predict theoretically the exact force between the sample and the tip. The results of this study support arguments for non-destructive imaging at molecular resolution under ambient conditions.

Molecular level defects observed in these images were stable with scan time and the lattice parameters obtained agree quite well with those obtained by other techniques such as x-ray diffraction and electron diffraction. The major source of error in lattice parameter measurements could be the small thermal and mechanical drift while scanning. Although we captured the images after 20-25 minutes of scanning, it is not possible to eliminate the drift completely. Surface roughness and composition (fused silica vs ITO) of the substrates do not seem to have any effect on the lattice parameter measurements. This suggests that atomically smooth surfaces such as mica, graphite or silicon wafers are not always necessary to obtain reliable molecular resolved images.

It was claimed that observation of well defined defects is a way to establish the achievement of true lateral atomic/molecular resolution[21]. The defects we observed were stable for long scanning times and for a variety of scanning directions with respect to the sample. Therefore we believe that we were imaging molecules. Also we tried to image a bilayer step with molecular resolution as is shown in Fig.10(a) in a 9 layer polymerized sample. To show the molecular resolution on both sides of the step, the dynamic scale was changed in this image (contrast enhancement); therefore, the gray scale does not give step height information. Fig. 10(b) shows the bearing plot (which is the height histogram with zero corresponding to the highest point in the image) for the entire image. The distance between the two peaks (5.745 nm), which is the height of the step, agrees with twice the length of a molecule. Except near the edge of the step, molecules are resolved in this image. Since this is a polymerized sample, one lattice direction (polymer backbone) is more pronounced than the other (see also Fig.5).

Fig 10(a) shows that polymerization takes place in the same direction in adjacent layers.

CONCLUSION

Lattice and defect structures of LB films of an unsaturated fatty acid, 12-8 diacetylene, have been studied by Scanning Force Microscopy. The lattice structure changed from a nearly centered rectangular lattice with lengths 0.88 ± 0.06 nm and 0.51 ± 0.04 nm to an oblique lattice with lengths 0.466 ± 0.008 nm and 0.55 ± 0.01 nm upon UV polymerization. We observed three different kinds of defects in these films which were stable with scanning time. Many researchers have argued, and it is still a puzzling question, that when the SFM is operating in ambient conditions, forces acting on soft samples may be too high and can damage the sample; hence, artifacts are possible and we may not see the real molecules. However, these results, especially the observed defects, suggest that we did image the real surface. These kinds of molecular level defects cannot be studied by techniques other than SFM. The results presented here demonstrate this capability.

Sharper tips would give lower operating forces due to a smaller contact area between the tip and sample. But in this work, pyramidal tips gave better results than sharper tips. This indicates that sharpness may have some limit in obtaining good molecular resolved images on soft samples as pointed out by Weihs

et al.[22]. Scanning under a suitable liquid will reduce the operating force by several orders of magnitude[27]. Experiments done in aqueous environment on 12-8 diacetylene LB films gave nearly the same lattice parameters[11,12] as we obtained in this work suggesting that it is possible to obtain reliable results on soft samples even scanning in air.

ACKNOWLEDGMENTS

This research was supported by the Advance Liquid Crystalline Optical Materials (ALCOM) program under Grant No. DMR-8920147 and Office of Naval research Grant No. N00014-94-1-01270.

REFERENCES

(1). "An Introduction to Ultrathin Organic Films from Langmuir-Blodgett to Self-Assembly", Abraham Ulman, Academic Press, Inc., San Diego, CA, (1991).

(2). "Langmuir-Blodgett Films", Gareth Roberts - Editor, Plenum Publishing Corporation, NY, (1990).

(3). F.Kajzar and J.Messier, Thin Solid Films, 99, 109(1983).

(4). J.Garnaes, D.K.Schwartz, R.Viswanathan and J.A.N. Zasadzinski, Nature, 357, 54(1992).

(5). D.K.Schwartz, J.Garnaes, R.Viswanathan, S.Chiruvolu and J.A.N. Zasadzinski, Phys. Rev. E, 47(1), 452(1993).

(6). J.P.K.Peltonen, P.He and J.B.Rosenholm, Langmuir, 9, 2363(1993).

(7). H.G.Hansma, S.A.C.Gauld, P.K.Hansma, H.E.Gaub, M.L.Longo and J.A.N. Zasadzinski, Langmuir, 7, 1051(1991).

(8). L.F.Chi, L.M.Eng, K.Graf and H.Fuchs, Langmuir, 8, 2255(1992).

(9). L.Bourdieu, P.Silberzan and D.Chatenay, Phy. Rev. Lett., 67(15), 2029(1991).

(10) Gtnter Lieser, Bernd Tieke and Gerhard Wegner, Thin Solid Films, 68, 77(1980).

(11). Constant A.J.Putman, Helen G.Hansma, Hermann E.Gaub and Paul K.Hansma, Langmuir, 8, 3014(1992).

(12). Babara M.Goettgens, Ralf W.Tillmann, Manfred Radmacher and Harmann E.Gaub, Langmuir, 8, 1768(1992).

(13). B.N.J.Persson, Chem. Phys. Lett., 141(4), 366(1987).

(14). Sun M.Paik, Sihong Kim and Ivan K.Schuller, Phys. Rev. B, 44(7), 3272(1991).

(15). Hemasiri Vithana, David Johnson, Raymond Shih and J. Adin Mann, Jr., Phys. Rev. E, 51(1), 454(1995).

(16). Landolt-Bornstein, Zahlenwerte und Funktionen; Springer, Berlin, 1(4), 109(1955).

(17). H.Heinzelmann, E.Meyer, D.Brodbeck, G.Overney and H.J.Gtntherodt, Z.Phys.B-Condensed Matter, 88, 321(1992).

(18). Bernd Tieke, Gtnter Lieser and Karin Weiss, Thin Solid Films, 99, 95(1983).

(19). K.Ogawa, H.Tamura, M.Hatada and T.Ishihara, Langmuir, 4, 903(1988).

(20). H.D.Gobel, H.E.Gaub and H.Mohwald, Chem. Phys. Lett., 138(5), 441(1987).

(21). F.Ohnesorge and G.Binnig, Science, 260, 1451(1993).

(22). T.P.Weihs, Z.Nawaz, S.P.Jarvis and J.B.Pethica, Appl. Phys. Lett., 59(27), 3536(1991).

(23). Nancy.A.Burnham, Richard.J.Colton and Hubert.M.Pollock, J. Vac. Sci. and Tech. A, 9(4), 2548(1991).

(24). Frank O.Goodman and Nicolas Garcia, Phys. Rev. B, 43(6), 4728(1991).

(25). Manfred.Radmacher, Karl. Eberle and Hermann.E.Gaub, Ultramicroscopy, 42-44, 968(1992).

(26). D.K.Schwartz, J.Garnaes, R.Viswanathan and J.A.N.Zasadzinski, Science , 257, 508(1992).

(27). A.L.Weisenhorn, P.Maivald, J.-H.Butt and P.K.Hansma, Phys. Rev. B, 45(19), 11226(1992).

FIGURE CAPTIONS

Fig. 1 (a)- Molecular resolved image of a polymerized diacetylene 9 layer film. (b)- 2D-Fourier spectrum of (a). Note that more than one set of spots are on one side of the spectrum due to the different lattice directions.

Fig. 2 (a)- Molecular resolved image of a monomer 9 layer diacetylene film. (b)- 2D-Fourier spectrum of (a). (c)- 2D-Fourier spectrum of an image of area of 16x16 nm^2. (d)- Schematic figure of the Fourier spectrum with miller indices.

Fig.3 Nearly centered rectangular, two-molecule unit cell corresponds to the lattice structure of the monomer diacetylene films as viewed from above. Alkyl chains are in a zig-zag plane and the dark spots correspond to the end methyl groups of the molecule.

Fig.4 2-dimensional auto correlation figure obtained from a molecular resolved image of monomer films. Note that the ordering extend more than 15 nm in all lattice directions.

Fig.5 (a)- Molecular resolved image of a polymerized 9 layer diacetylene film. (b)- 2D-Fourier spectrum of (a).

Fig.6 2-dimensional auto correlation figure obtained from a molecular resolved image of polymerized films. Ordering extend more than 15 nm in both lattice directions.

Fig.7 (a)- Image of a grain boundary observed in a 9 layer monomer film. Angle between the misoriented lattice directions is ~ 9^0. Note that the row of molecules at the boundary is not well resolved compared to the molecules in the two domains. (b)- 2D-Fourier spectrum of (a). Values of the wave vectors corresponding to the two spots are also indicated.

Fig.8 Image of dislocations and a low angle grain boundary observed in a 9 layer monomer film. This image is Fourier filtered by keeping only the intense spots in the 2D-Fourier spectrum.

Fig.9 (a)- Image of screw dislocations observed in a 9 layer polymerized film. (b)- Cross sectional profile across the line drawn in (a). Height between the two marks in the figure, which is the height of the slipped film is 5.613 nm.

Fig.10 (a)- Molecular resolved image of a bilayer step observed in a 9 layer polymerized film. Dynamic scale was changed in this image to show the resolution in both steps; the gray scale does not corresponds to height values. (b) Bearing curve of the entire image (a). This is the height histogram of the picture with zero height corresponds to the highest point in the image. Distance between the two peaks is 5.745 nm.

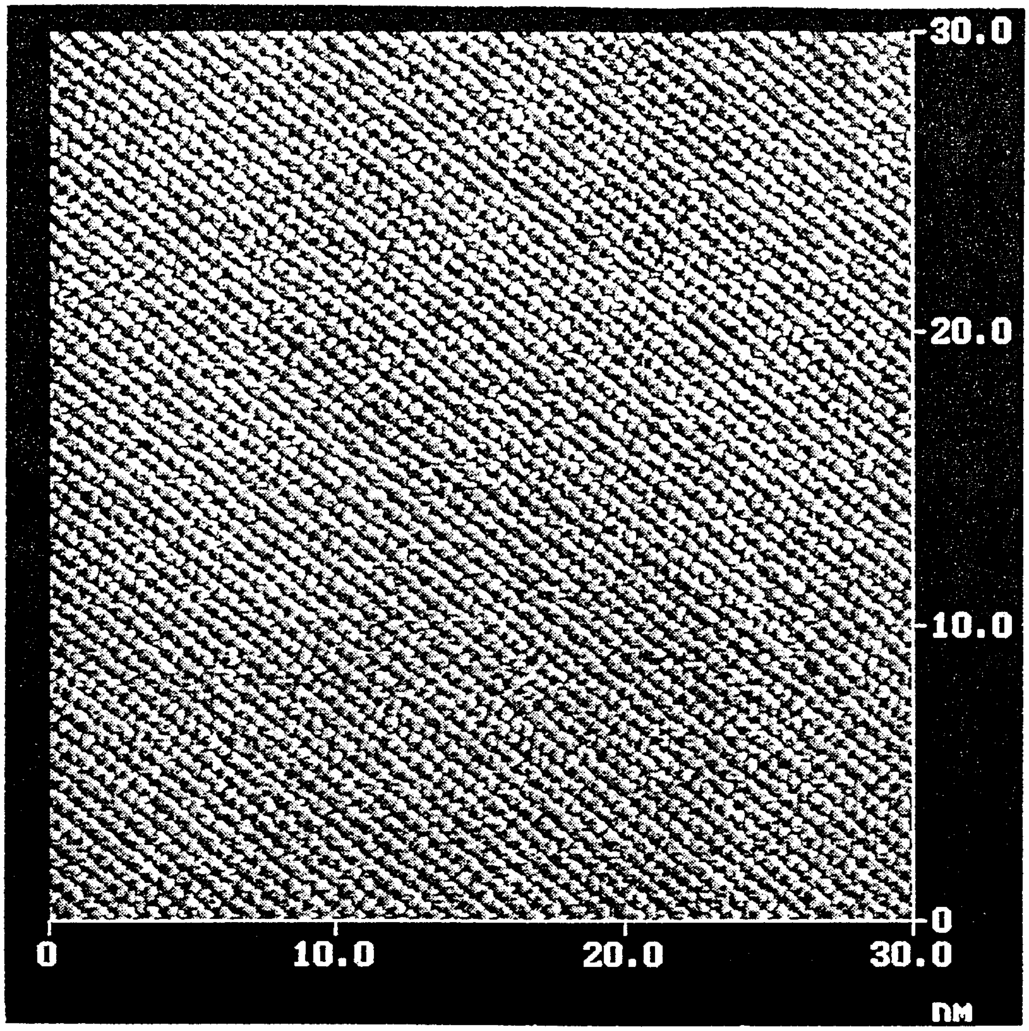

Vithana et al., Fig 1 (a)

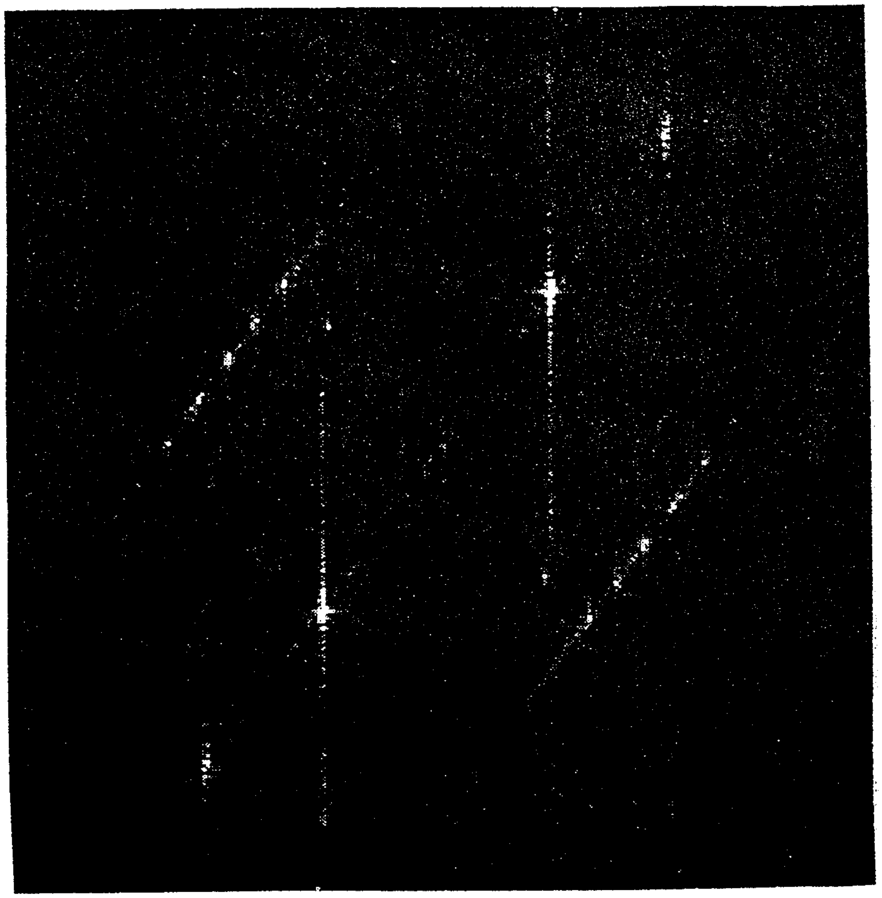

Vithana et al.,

Fig 1 (b)

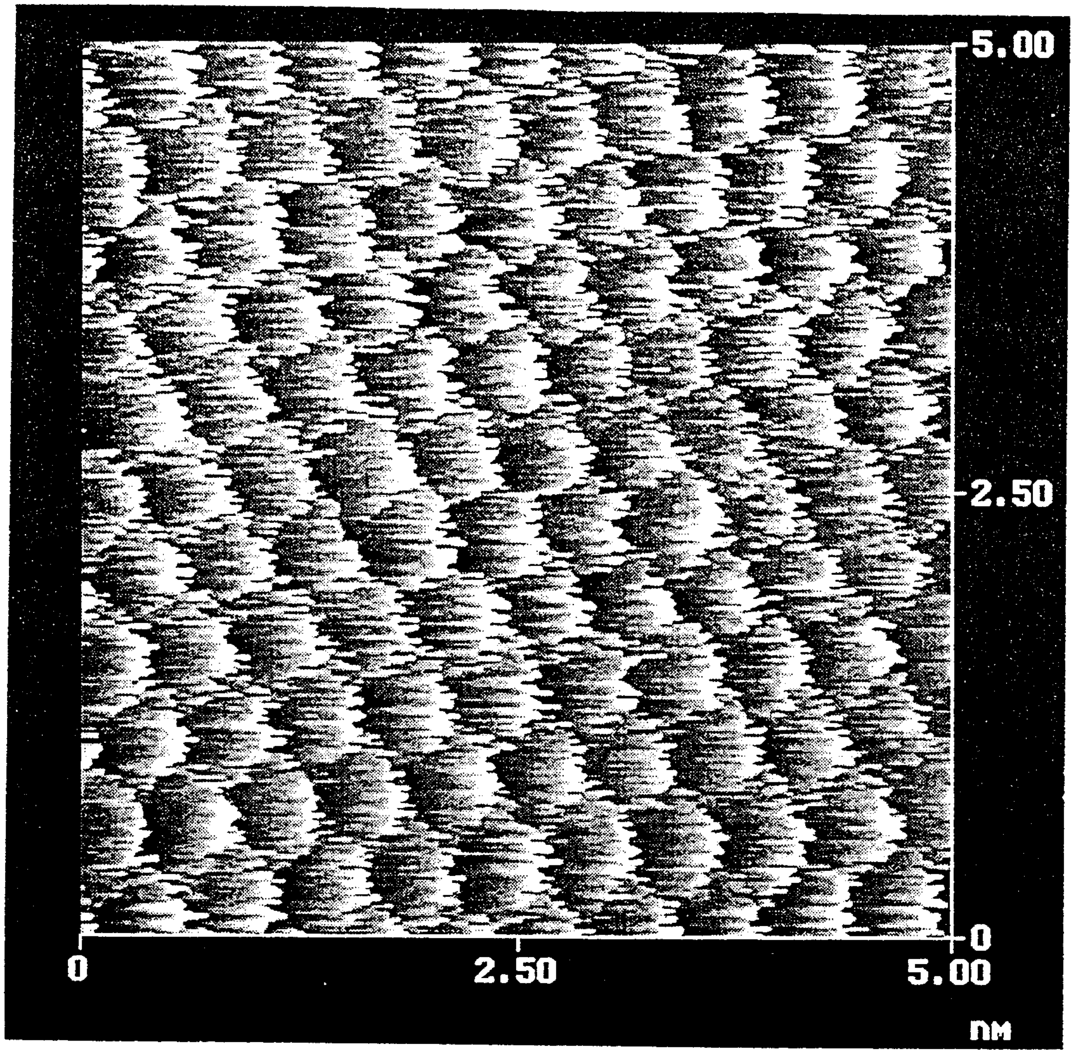

Vithana et al.,

Fig. 2 (a)

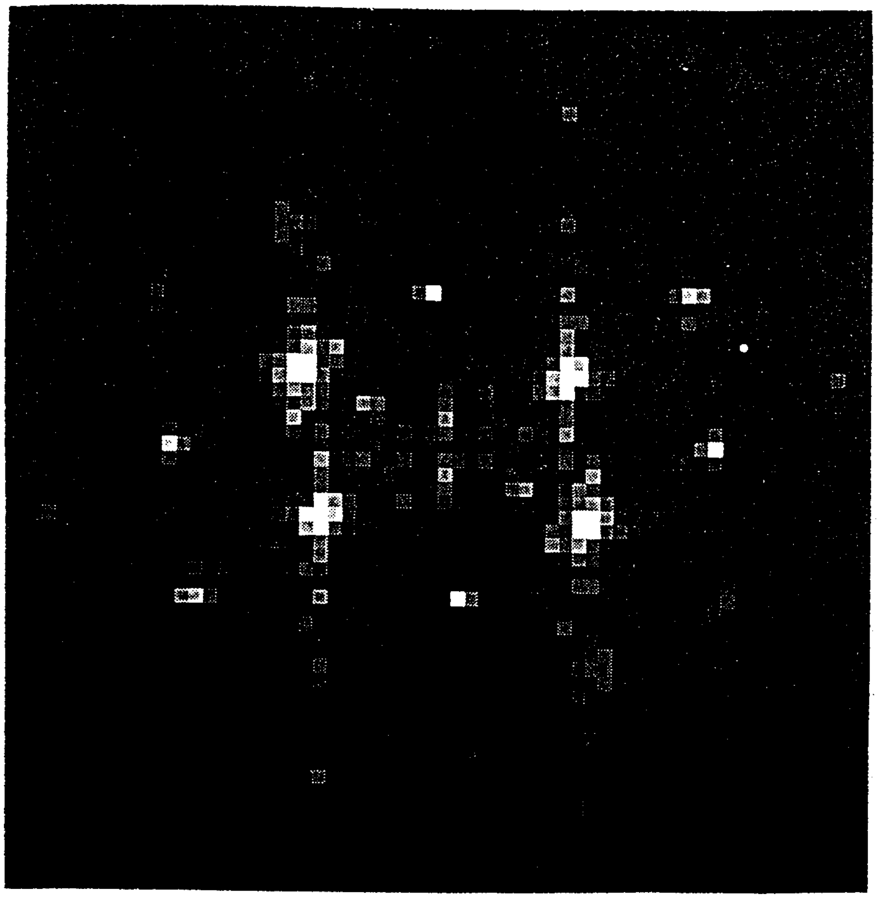

Vithana et al., Fig 2 (b)

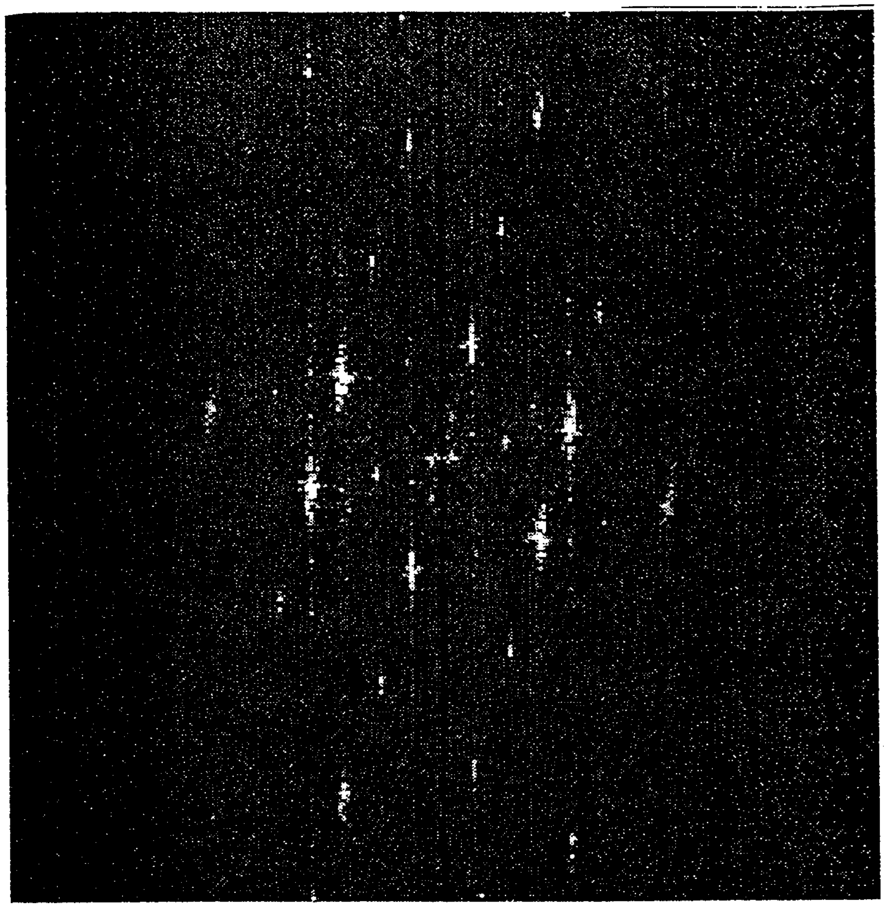

Vithana et al.,

Fig 2 (C)

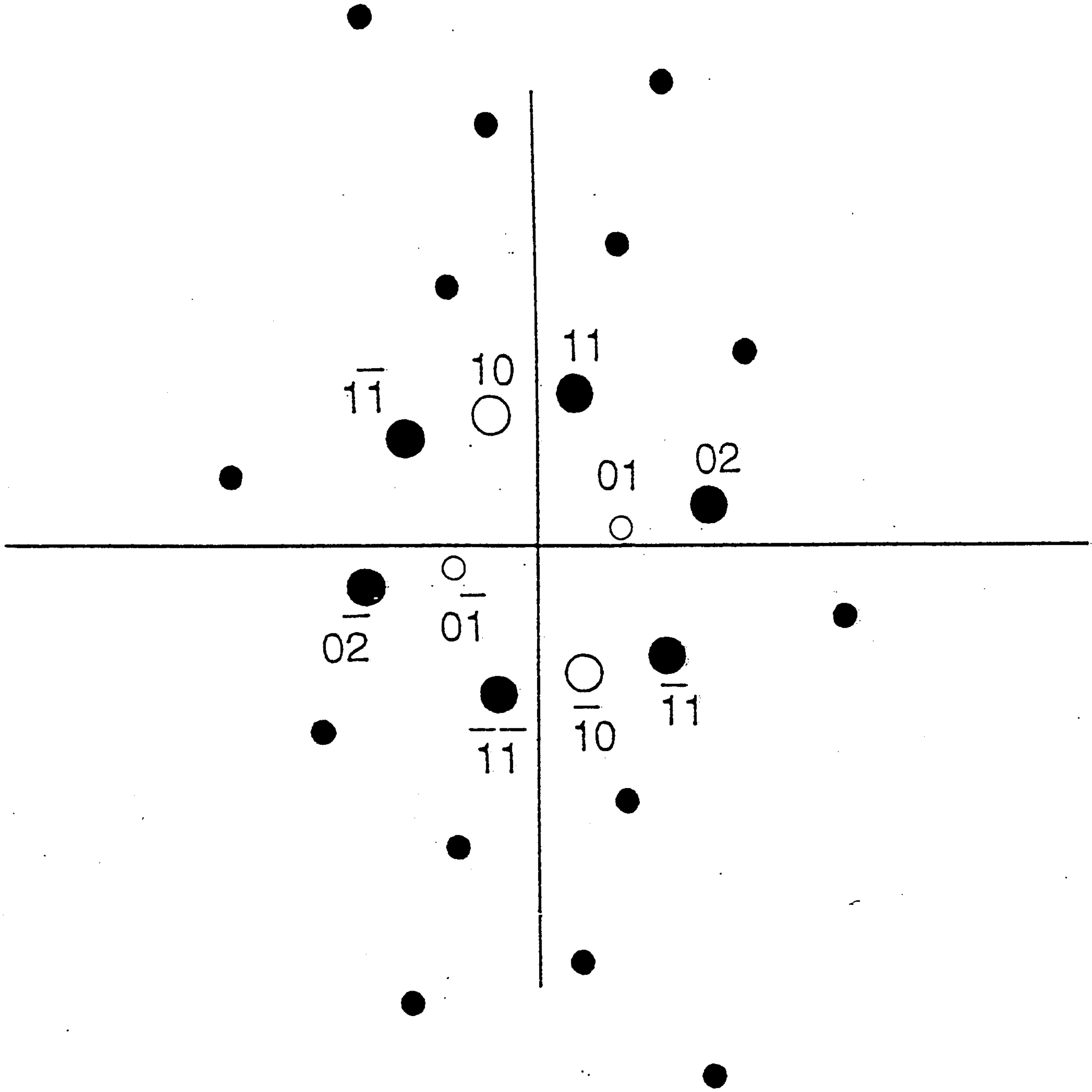

Vithana et al.,

Fig. 2 (d)

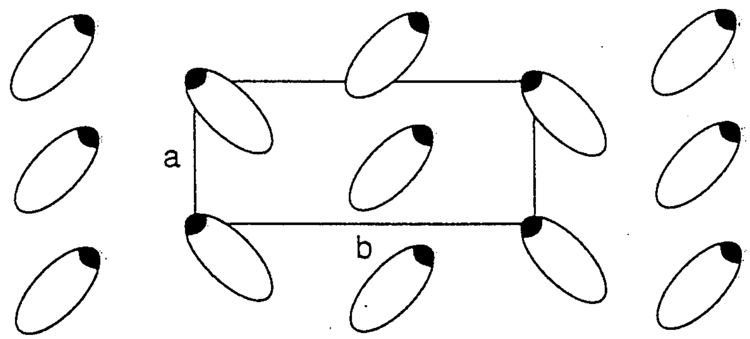

Vithana et al.,

Fig. 3

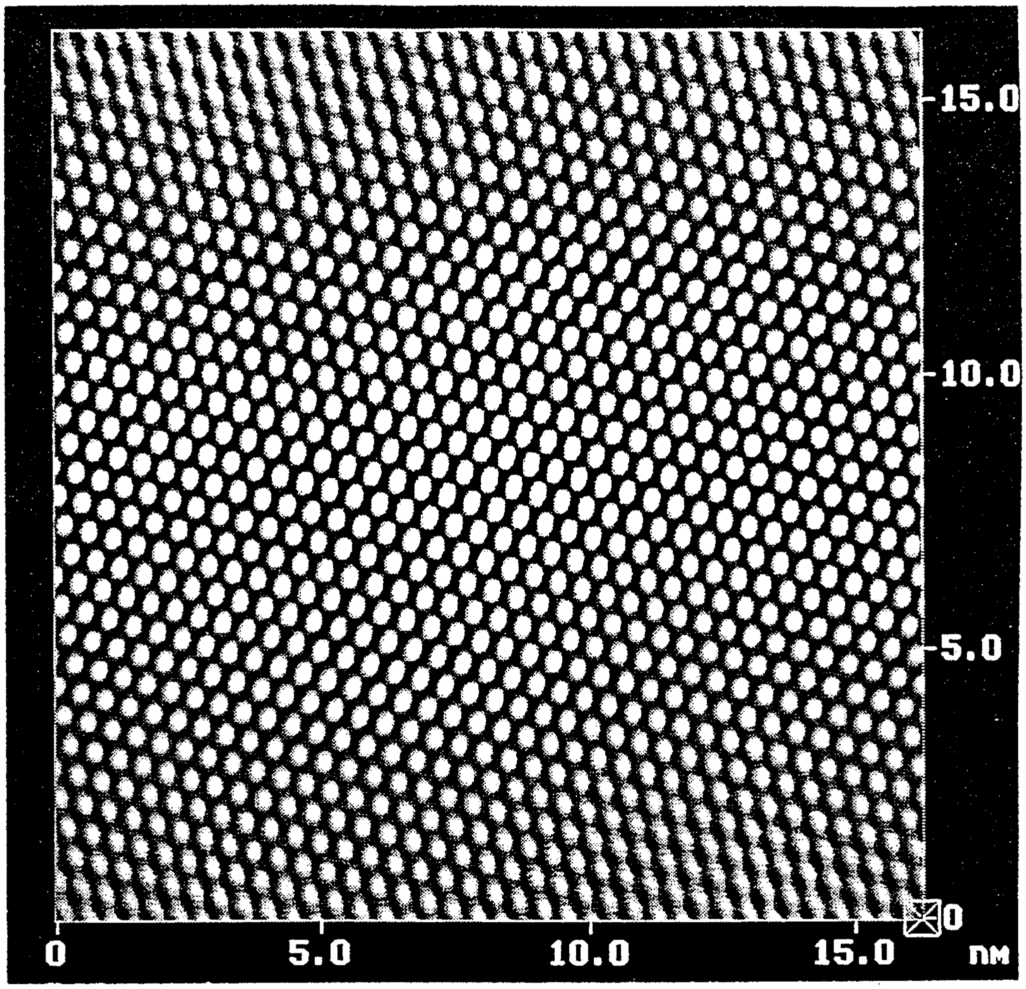

Vithana et al.,

Fig. 4

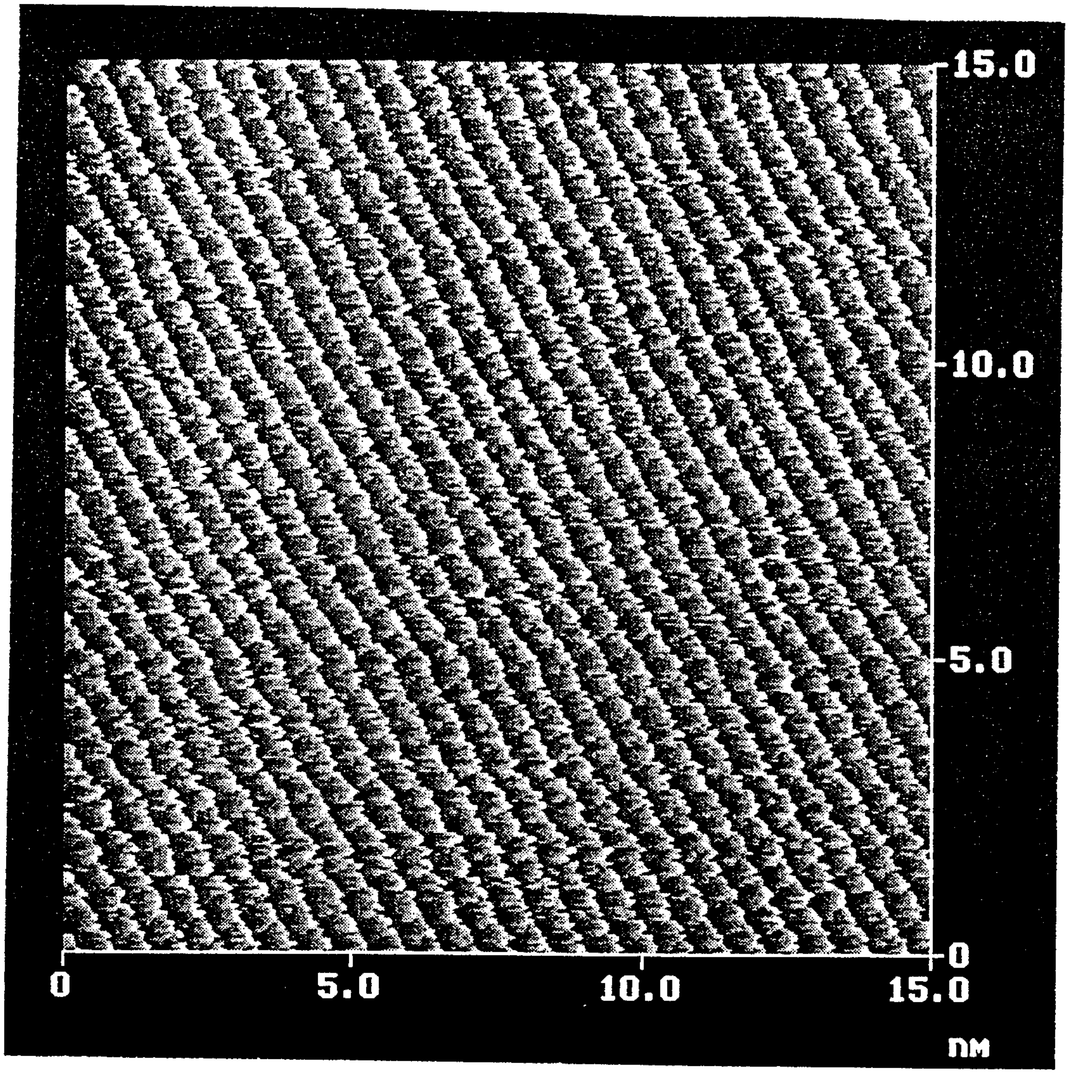

Vithana et al.,

Fig. 5(a)

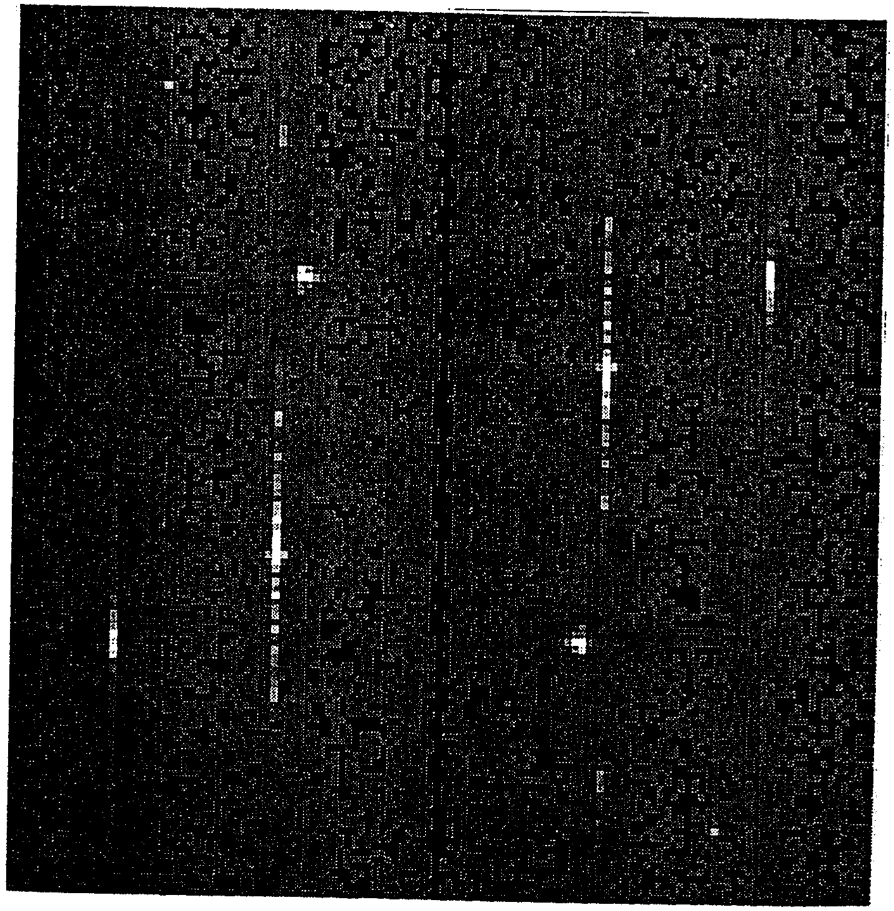

Vithana et al.,

Fig. 5(b)

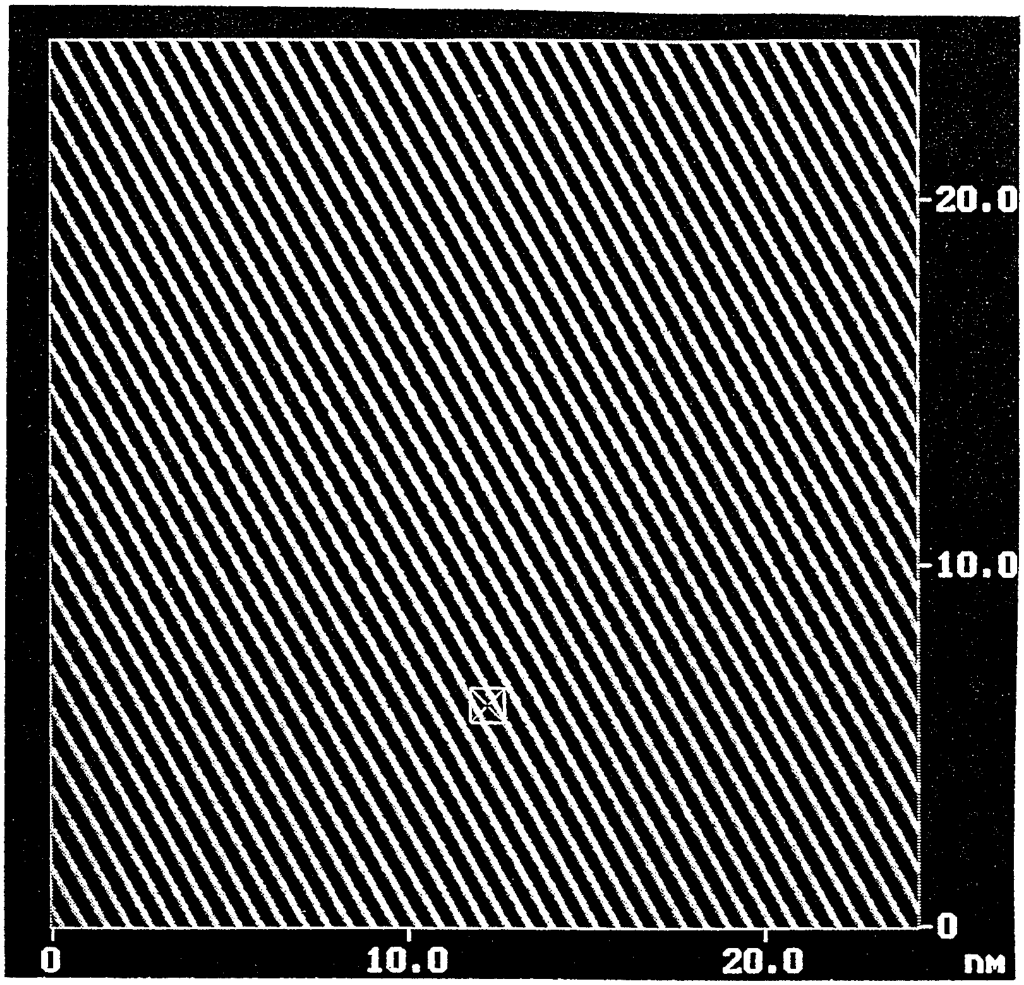

Vithana et al., Fig. 6

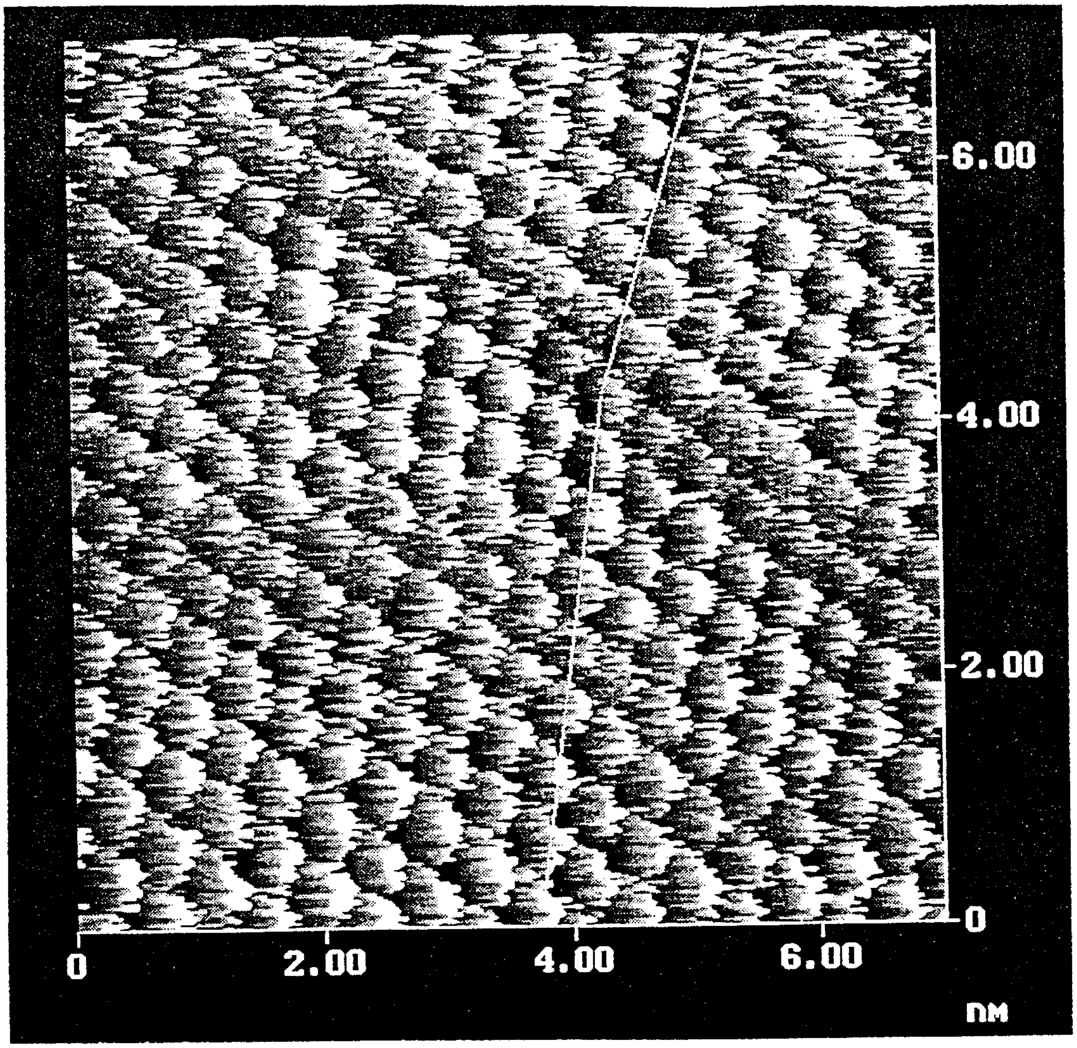

Vithana et al.,

Fig. 7 (a)

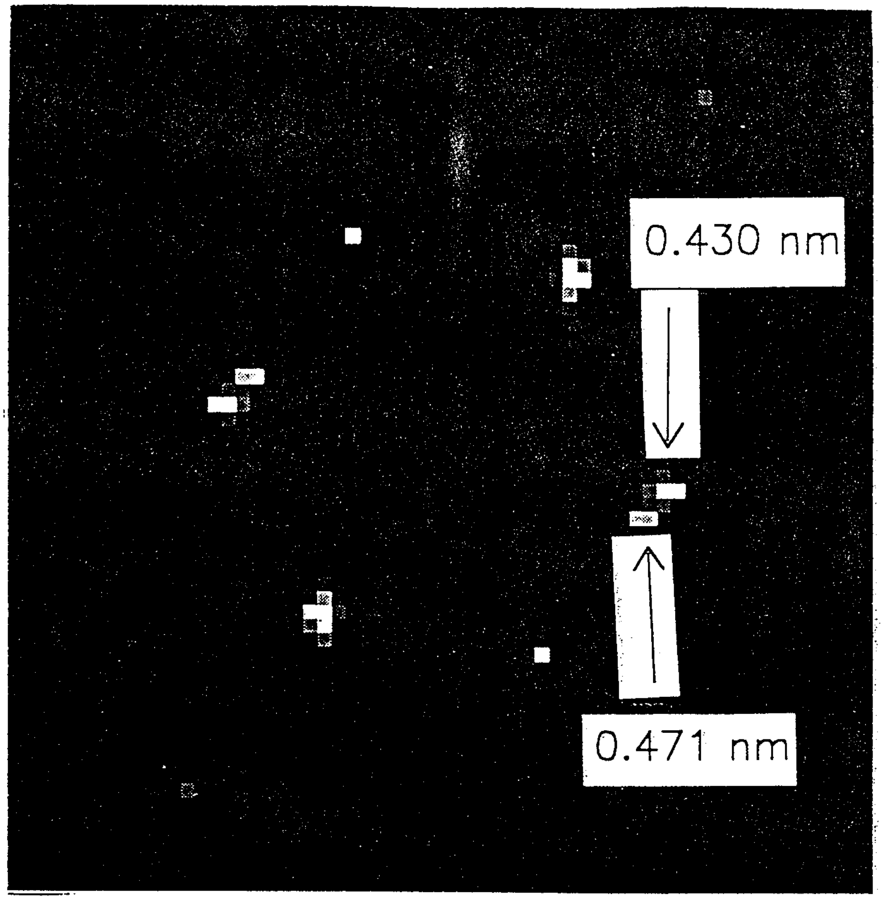

Vithana et al.,

Fig. 7(b)

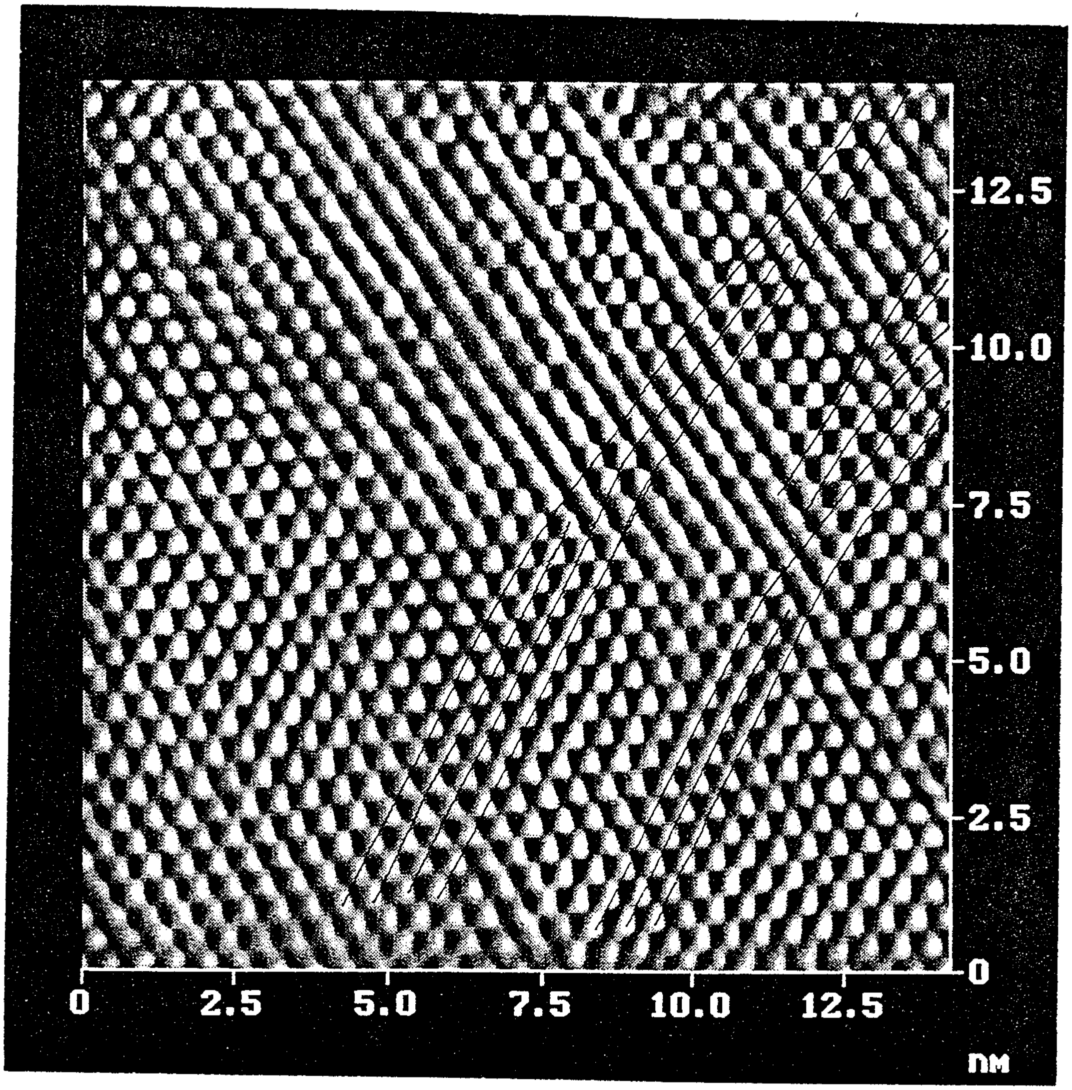

Vithana et al.,

Fig. 8

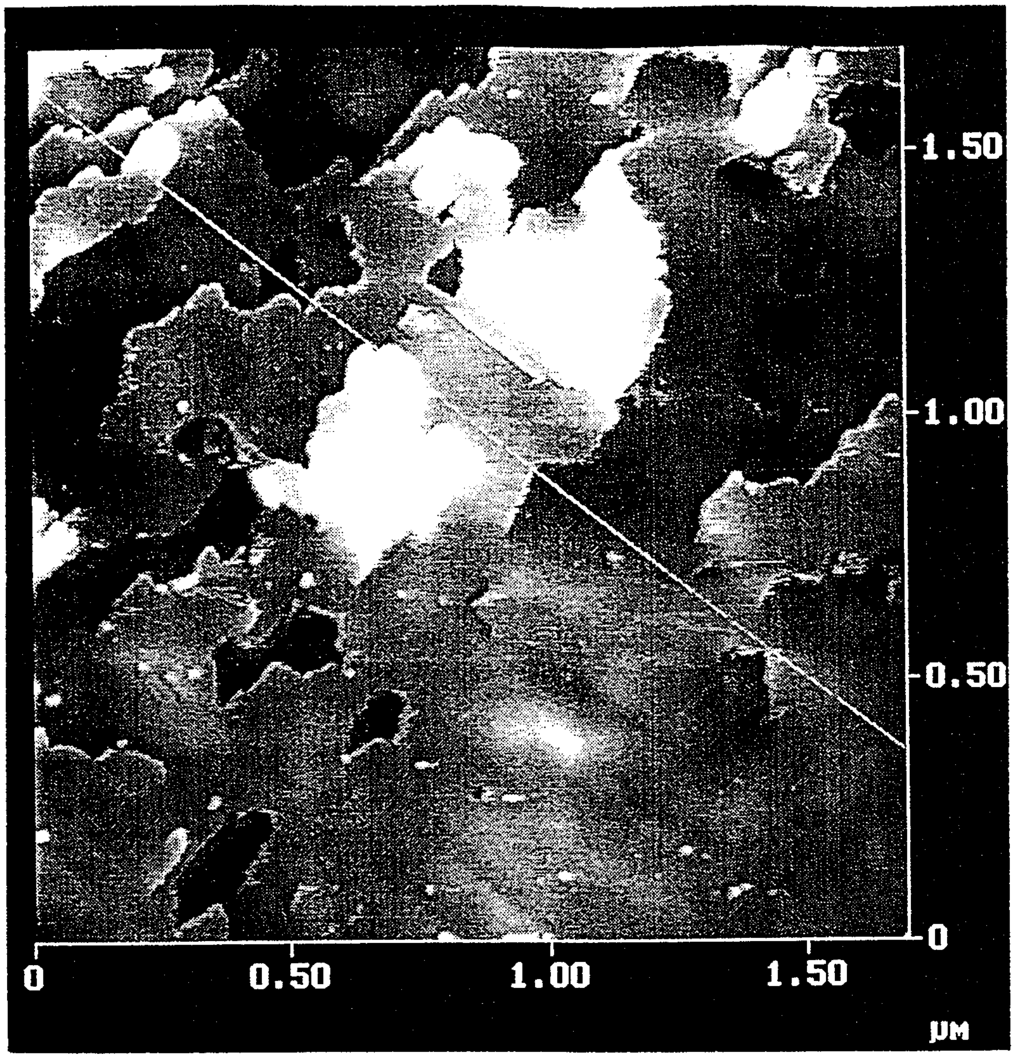

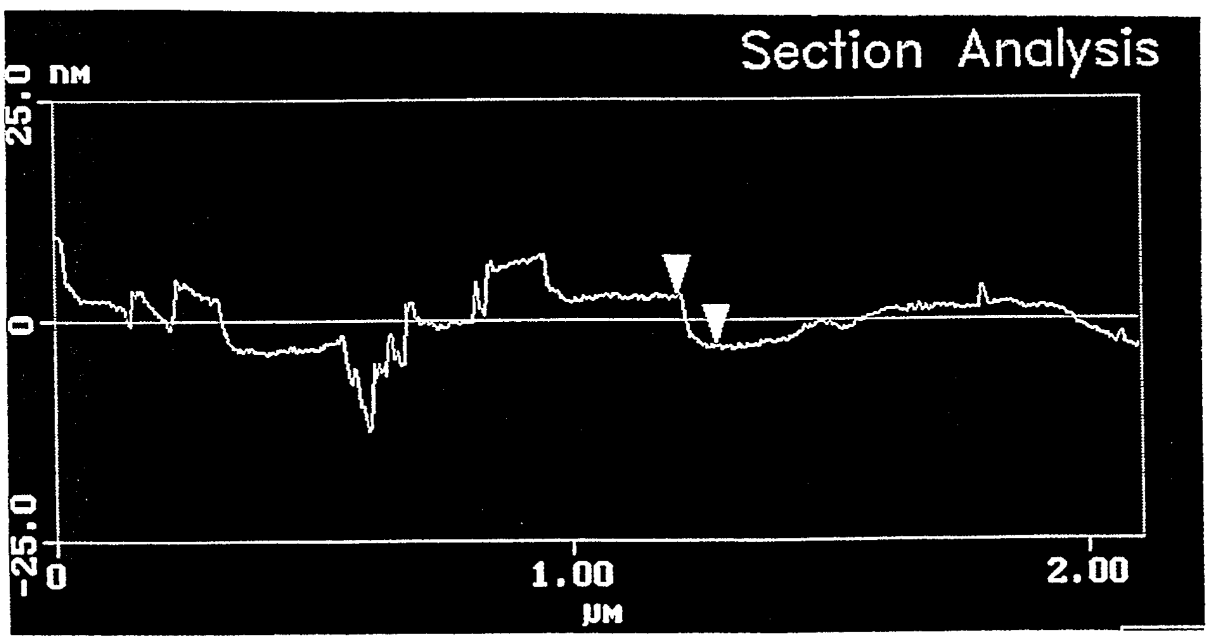

Vithana et al.,

Fig 9(a) and 9(b)

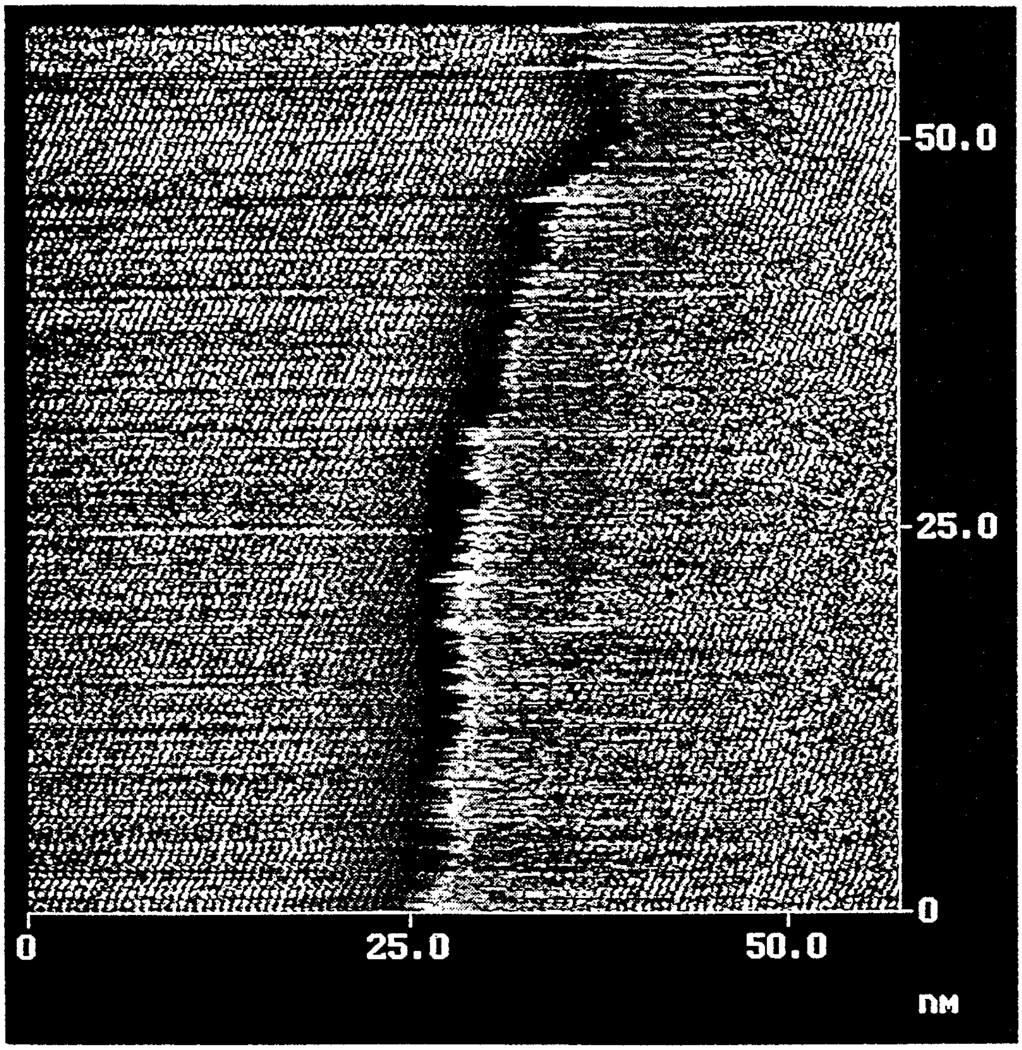

Vithana et al.,

Fig. 10(a)

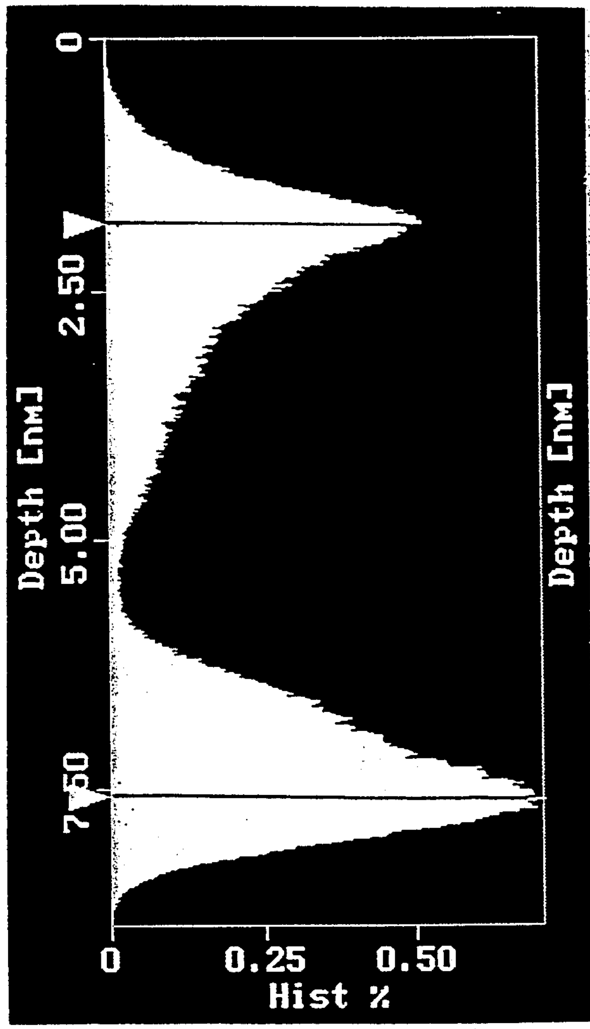

Vithana et al.,

Fig. 10(b)